Journal of Applied Electrochemistry **34**: 337–343, 2004.

Characterization of different allotropic forms of calcium carbonate scales on carbon steel by electrochemical impedance spectroscopy

J. MARÍN-CRUZ[1,2], R. CABRERA-SIERRA[1,3], M.A. PECH-CANUL[4] and I. GONZÁLEZ[1,*]
[1]*Universidad Autónoma Metropolitana, Departamento de Química. Apdo. Postal 55-534, 09340 Mexico, D.F., Mexico*
[2]*Instituto Mexicano del Petróleo, Coordinación de Ingeniería Molecular, Área de Materiales y Corrosión, Eje Central Lázaro Cárdenas No. 152, C.P. 07730, D.F., Mexico*
[3]*Escuela Superior de Ingeniería Química e Industrias Extractivas (ESIQIE-IPN), Academia de Química Analítica, Edificio Z5. A.P:75-874, C.P. 07338, D.F., Mexico*
[4]*Departamento de Física Aplicada, Centro de Investigación y de Estudios, Avanzados del IPN, A.P. 73 Cordemex, C.P. 97310, Mérida, Yucatán, Mexico*
*(*author for correspondence, fax: +52 55 5804 4666, e-mail: igm@xanum.uam.mx)*

Received 6 January 2003; accepted in revised form 6 November 2003

Key words: aragonite, calcite, calcium carbonate scales, carbon steel, electrochemical impedance spectroscopy

Abstract

Calcium carbonate scales with allotropic forms of aragonite, calcite and a mixture of both, were selectively induced onto carbon steel substrates in a synthetic cooling water. Electrochemical impedance spectroscopy (EIS) was successfully applied to characterize these scales. The resistance and capacitance of the high frequency loop of impedance diagrams for the aragonite and aragonite–calcite scales were related to the morphology of the deposits, and gave information which is in good agreement with scanning electron microscopy (SEM) observations. The impedance response of the scale with a calcite–aragonite mixture was dominated by the aragonite constituent. However, the calcite constituent has a strong influence on the scale morphology, so that the calcite crystals merged laterally with the aragonite agglomerates to form a more coherent and thicker scale, compared to that for a scale consisting of aragonite alone. For scales containing aragonite and a calcite-aragonite mixture, increasing the formation time lead to less porous and thicker deposits.

1. Introduction

Scaling is one of the potential problems associated with industrial systems using fresh water for heat removal. The scale deposit leads to a deterioration in thermal performance of heat exchangers and produces regions on heat transfer surfaces that are ultimately susceptible to localized corrosion. Potential scale deposits are usually related to calcium and magnesium salts in the presence of high concentrations of ions such as: CO_3^{2-}, PO_4^{3-}, SO_4^{2-}, and SiO_3^{2-}. Calcium carbonate is the most predominant scaling constituent in cooling water systems. Three major $CaCO_3$ polymorphs, namely, calcite, aragonite and vaterite have been identified in scales [1, 2], although vaterite is very rare [1, 3, 4]. Since the morphology and crystal habit of the deposits determine important properties such as thermal conductivity, compactness, and tendency for removal, it is of high priority to systematically investigate how the morphology and growth pattern of $CaCO_3$ deposits may be affected or induced under well-controlled conditions.

Electrochemical deposition provides a good way of simulating calcium carbonate crystallization at metal surfaces. Numerous studies have appeared using this method to investigate scaling kinetics [5–8], nucleation/growth mechanisms [9–11], structure [12, 13] and morphological features of deposits [2, 5, 7, 12, 13]. In most of these studies noble metal substrates and synthetic water containing mainly Ca^{2+} and HCO_3^- ions, have been used. However, it has been shown [2] that water composition influences the polymorphic formation of calcium carbonate and the nature of the substrate affects the morphology and scaling rate. Thus, investigations of scaling using substrates and water compositions relevant to practical cooling water systems are still needed.

In previous studies [14, 15], calcium carbonate scales with allotropic forms of aragonite, calcite and a mixture of both, were selectively induced onto carbon steel substrates in synthetic cooling water (simulating the typical composition of cooling water used in Mexican oil refineries) in a reproducible and controlled fashion. The degree of electrode coverage by aragonite and calcite scales was evaluated using cyclic voltammetry [15]. The aim of this paper is to characterize the three scale deposits (aragonite, calcite and mixture of both) using electrochemical impedance spectroscopy (EIS).

2. Experimental details

The experiments were carried out in a model cooling water (identified as AS3C) which simulates the average composition of cooling waters used in Mexican oil refineries, as follows: 3.0×10^{-3} M $CaCO_3$ [360 ppm Ca(II)]; 1.5×10^{-3} M $MgCl_2 \cdot 6\ H_2O$ [150 ppm Mg(II)]; 8.3×10^{-4} M SiO_2 [50 ppm SiO_2]; 4.0×10^{-3} M Na_2SO_4 [200 ppm SO_4(−II)]; 2.6×10^{-3} M NaCl [200 ppm Cl(−I)]; 1.1×10^{-3} M NaH_2PO_4 [10 ppm PO_4(−III)] and 3.6×10^{-6} M $FeSO_4 \cdot 7\ H_2O$ [0.1 ppm Fe(II)]. The pH was adjusted to 7.8 and the temperature was maintained at 40 °C.

A 1018 carbon steel rotating disc electrode with a surface area of 0.5 cm^2 was used in a typical three-electrode cell. A saturated calomel electrode (SCE) was the reference electrode, and the counter electrode was a graphite bar, both arranged within a separate compartment. The surface of the disc electrode was mechanically polished with silicon carbide emery paper (no. 600), and then washed in an ultrasonic bath in acetone for 5 min. A 283-model PAR potentiostat/galvanostat was used alone (for electrochemical deposition of the scales) or connected with a computer-controlled 1250 Solartron frequency response analyser for electrochemical impedance measurements.

2.1. *Scale induction*

Different extents of scaling were induced on the surface of steel electrodes rotating at 2000 rpm in the AS3C model water, through direct potential pulses in three potential regions, as reported previously [14, 15]. The scales consisted of calcite (at −1.75 V vs SCE), of aragonite (at −1.1 V vs SCE) and a mixture of calcite–aragonite (at −1.3 V vs SCE). Although both reduction reactions were carried out simultaneously, the potentials −1.1 and −1.3 V vs SCE correspond mainly to oxygen reduction, while −1.75 V vs SCE predominantly corresponds to water reduction. Because of the strong hydrogen evolution at more negative potentials (calcite scale formation), an effect on scale adhesion and stability is expected and this effect is responsible for the lower adherence of the calcite formed in the AS3C solution. Unfortunately, for the chemical composition used in this work, calcite cannot be electrochemically induced at less negative potentials, as other authors claim [12], to avoid hydrogen evolution and increase scale adhesion. A more detailed description of scale induction is reported elsewhere [14]. The extent of scale was controlled through the duration of the potential pulse (generally 5 min).

2.2. *Characterization of scales*

Characterization by EIS involved the determination of the typical impedance response of scaled electrodes when immersed in a fixed characterization medium. For this purpose, fresh AS3C model water was chosen. Thus, in each case the scale was formed at its corresponding potential (e.g., calcite at −1.75 V) and at the end of the 5 min potential pulse the AS3C solution was

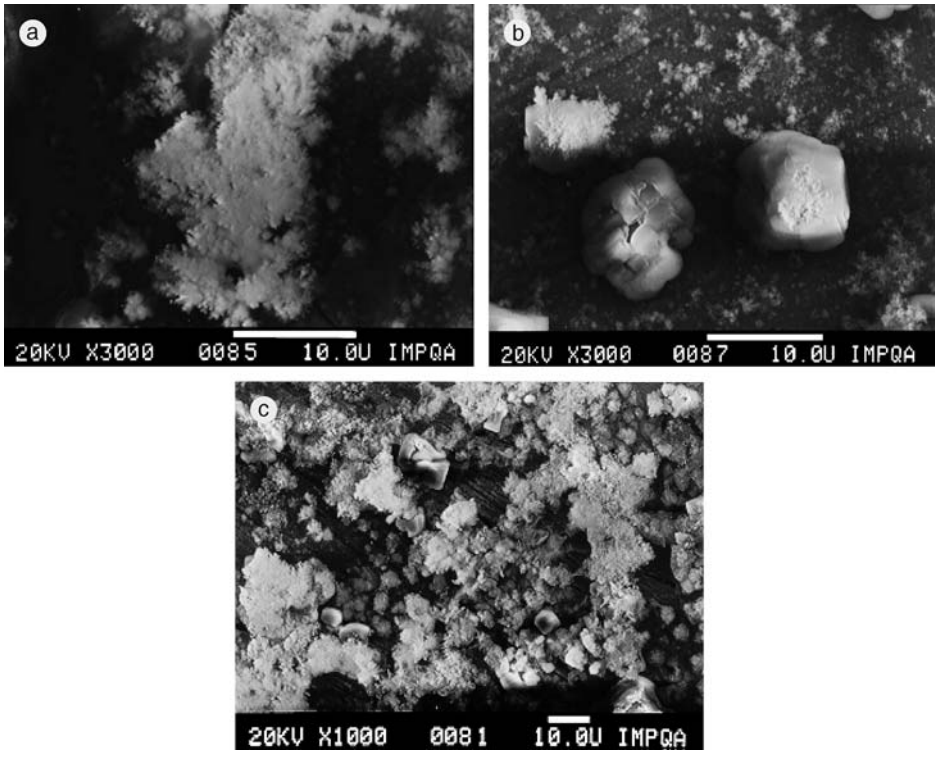

Fig. 1. SEM images of carbon steel surfaces scaled with different calcium carbonate allotropic forms: (a) aragonite, (b) calcite and (c) aragonite–calcite mixture. The scales were obtained in the AS3C solution by polarizing the electrode at −1.1, −1.75 and −1.3 V vs SCE, respectively.

replaced by a fresh one. The scaled electrodes continued rotating at 2000 rpm in the fresh solution and, after a stabilization time of 10 min, electrochemical impedance measurements were carried out at the corrosion potential, using a signal of 10 mV amplitude in a frequency interval ranging from 50 kHz to 10 mHz, with 10 steps decade^{-1}.

Selected samples were examined using X-ray diffraction (XRD) and/or Scanning Electron Microscopy (SEM) immediately after damage induction. SEM was carried out using a Jeol model JSM-35CF equipment and by XRD in a microcrystal Siemens Daco MP diffractometer.

3. Results and discussion

3.1. *SEM and XRD characterization of scaled surfaces*

Figures 1(a)–(c) show typical SEM images corresponding to steel surfaces scaled in the AS3C (formation time 5 min) solution at −1.1 V vs SCE, −1.75 V vs SCE and −1.3 V vs SCE, respectively. Figure 1(a) shows agglomerates with a dendritic growth pattern, typical of aragonite crystals. The porous nature of the deposit is evident. Figure 1(b) shows relatively large, isolated, rhombohedral calcite crystals surrounded by fine grains next to the substrate. For these crystals an edge-rounding effect is observed, which could be due to the incorporation of magnesium ions into the calcite crystal lattice [1, 12]. Figure 1(c) shows a mixture of calcite crystals and aragonite agglomerates, which seem to merge laterally to form a more coherent deposit compared to that for aragonite (a) or calcite (b) alone.

Figure 2(a) shows the diffraction spectrum of the scale formed at −1.75 V vs SCE. The comparison of the experimental spectrum and the reference pattern of calcite (solid line, Figure 2(a)) confirms that the electrochemically formed crystals consist mainly of calcite. Figure 2(b) shows the XRD spectrum for the scale formed at −1.3 V vs SCE. Both structures of calcium carbonate (aragonite and calcite) are present. However, the scale contains mainly the aragonite form, as indicated by the intensity of peaks at 2θ angle of 26.2°, 27.3° and 46.0° [12]. For the scale formed at −1.1 V vs SCE, the presence of aragonite was not detected in the XRD pattern (even when the low angle technique was used), probably due to the highly amorphous structure of the scale.

Although the model water contained Mg ions, it was not possible to identify magnesium hydroxide, which is expected to be formed in the initial stages of scaling

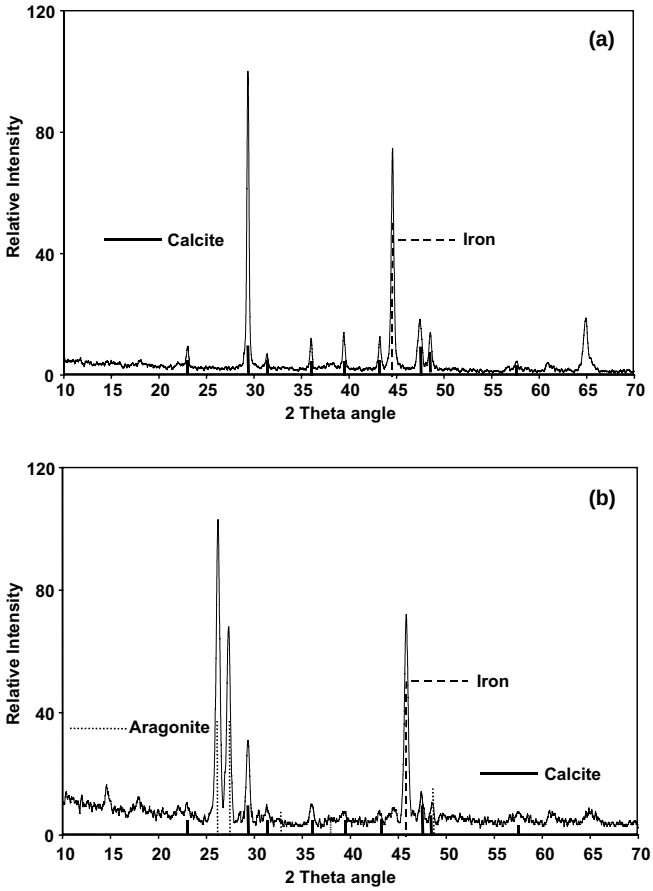

Fig. 2. XRD spectra of scales formed on carbon steel surface with different potential pulses, in the AS3C solution at pH 7.8 and 40 °C. (a) scale formed at −1.75 V, and (b) scale formed at −1.3 V vs SCE. Different XRD patterns are indicated in the figure: (– – –) carbon steel reference surface, (—) calcite and (·····) aragonite.

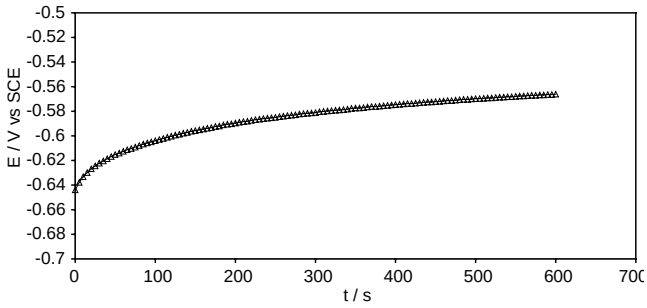

Fig. 3. Variation of corrosion potential (E_{cor}) against immersion time in fresh solution AS3C (characterization medium) of a scaled carbon steel surface (aragonite previously grown for 10 min). Electrode rotation rate 2000 rpm.

[16, 17]. However, it has also been reported that the Mg content in the scale significantly diminishes with increasing temperature [16], or SO_4^{2-} ions in the solution [17]. In this work the experimental conditions for scale induction were a temperature of 40 °C and a concentration of SO_4^{2-} ions of at least 4×10^{-3} M.

3.2. *Impedance response of scaled and unscaled steel in AS3C solution*

The information gained from EIS would be meaningless if the stability requirement were not satisfied. Corrosion potential monitoring showed that in the AS3C model water, 10 min stabilization was enough before starting the EIS measurement both for scaled and unscaled (those immersed in the characterization medium right after the polishing/cleaning procedure) electrodes. Such behaviour is illustrated in Figure 3 for an electrode previously scaled with aragonite at −1.1 V and then immersed in a fresh AS3C solution. Although the graph shows only data for 10 min, the stability was maintained long enough to perform a frequency sweep from 100 kHz down to 0.01 Hz.

Figure 4 shows the impedance diagram for a steel electrode that remained 10 min at open circuit conditions in the AS3C solution (at 2000 rpm). Since no scale was induced electrochemically on the surface, the impedance response is that of the steel/corrosion products/water system. The Nyquist diagram seems to consist of three loops, although the low frequency (LF) one is poorly resolved. The high frequency (HF) loop resembles a capacitive semicircle, and an evaluation of its capacitance (C_{HF}) from the diameter (R_{HF}) of the semicircle and its characteristic frequency gives a value of about 8 μF cm^{-2}. The small value of C_{HF} compared to the typical 50 μF cm^{-2} for a double layer capacitance, as well as the small value of $R_{HF,}$ makes it difficult to ascribe this loop to the charge transfer process. The most plausible explanation, in agreement with observations of other authors [18, 19], is that it corresponds to the porous layer of corrosion products formed at the metal surface. Thus, the medium (MF) and LF frequency loops represent the faradaic process which takes place on the surface uncovered by such a layer.

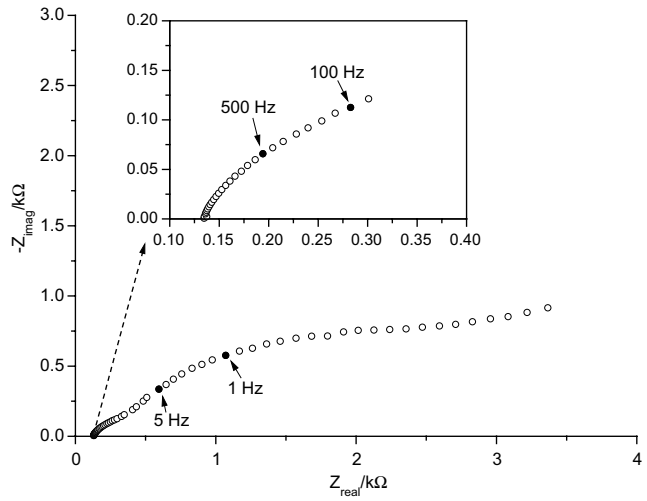

Fig. 4. Impedance spectrum obtained for a carbon steel electrode that remained 10 min at open circuit conditions in the AS3C solution (at 2000 rpm). No damage was induced electrochemically on the surface (i.e., unscaled surface). The inset shows the data obtained at high frequencies.

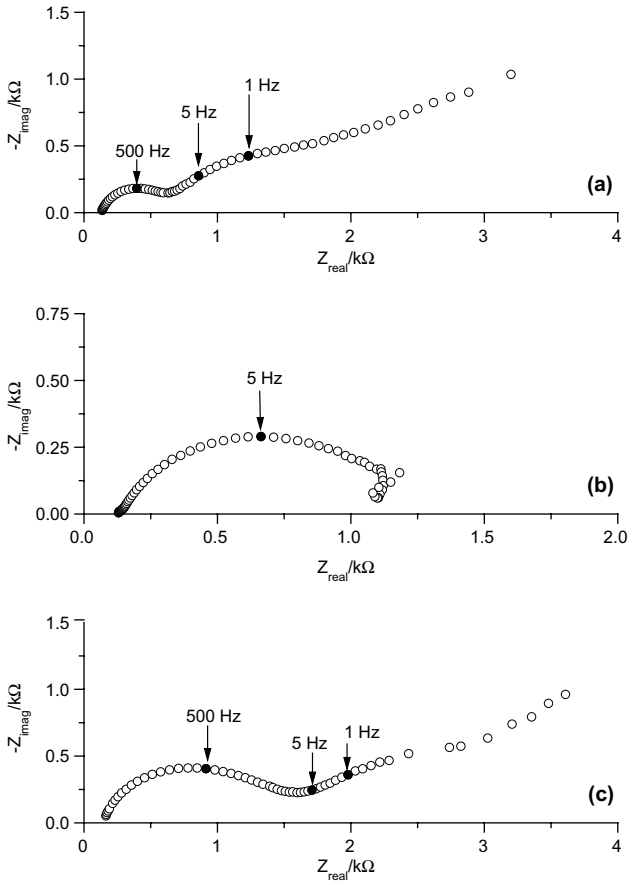

Fig. 5. Typical impedance diagrams obtained after 10 min in fresh AS3C solution (characterization medium), for surfaces that were previously scaled (5 min formation time) with: (a) aragonite, (b) calcite and (c) aragonite–calcite mixture.

Figures 5(a)–(c) show the impedance spectra obtained after 10 min in fresh AS3C solution, for surfaces that were previously scaled (5 min formation time) with aragonite, calcite and an aragonite–calcite mixture, respectively. The Nyquist diagram for aragonite in Figure 5(a) exhibits three loops where the HF one is a semicircle with a characteristic capacitance of about 1 μF cm^{-2}. For the unscaled electrode C_{HF} was ascribed to a corrosion product layer. In this case, it corresponds to the aragonite scale itself, since electrochemical conditions of scale formation assured negligible presence of corrosion products. The HF arc in Figure 5(a) is larger, more clearly defined and with a lower capacitance, compared to that in Figure 4, thus suggesting that the aragonite scale is relatively more compact, and possibly thicker, than the layer of corrosion products. The MF and LF loops in Figure 5(a) can be ascribed to the faradaic process taking place on the surface uncovered by the aragonite scale. This process is oxygen reduction and a hypothesis can be put forward that the MF loop is related to the charger transfer process and the LF one is related to molecular diffusion. A test of rotation rate effect (Figure 6) shows that the impedance diagram area is almost unmodified, thus suggesting that convective flow effect is negligible and oxygen diffusion through the compact scale layer is responsible for the LF impedance response. The MF loop in Figure 5(a) is highly depressed and the most likely explanation is that there is a distributed ohmic drop across the scale layer. Similar behaviour was observed by Gabrielli and coworkers [2, 7] who proposed that for a scaled electrode oxygen diffuses through the porous layer and reduction occurs in cavities under the blocks of scale crystals. These authors derived an impedance model which takes into account partially blocked electrode phenomena and transmission line-effects.

The calcite layer exhibited a distinct impedance response (Figure 5(b)). Gabrielli et al. [7] investigated calcite scales formed on platinum rotating electrodes in carbonically pure water. Their impedance spectra exhibited a response typical of transmission line impedance and were analysed accordingly. The impedance diagram in Figure 5(b) does not exhibit such behaviour. Even though in both works calcite layers were present, it is possible that the morphology and adherence of the deposit was different due to the difference in substrates, as pointed out recently by Gabrielli and coworkers [2], and the potential required for the calcite formation, with hydrogen evolution having a possible influence at more negative potentials [14]. Comparing the impedance response of the calcite scale in this work, to that for an aragonite scale, the HF loop disappeared, the MF loop became more like a capacitive semicircle (slightly depressed), and the LF loop turned into an inductive feature. The fact that the impedance diagram in Figure 5(b) does not exhibit a HF arc is possibly because the calcite crystals are not closely packed to form a coherent layer, but remain isolated. Based on the literature on electrodeposition of metals [20–22], the inductive effect could be related to a relaxation of the surface layer through desorption or dissolution processes.

The impedance response for the aragonite–calcite mixture (Figure 5(c)) is similar to that for the aragonite scale, except that the HF loop is larger and there is a slight shift in the characteristic frequencies of the HF and MF arcs. According to the characterization with SEM, the calcite crystals merge laterally with the aragonite agglomerates to form a more coherent scale. This explains the larger size and smaller capacitance (about 0.3 μF cm^{-2}) of the HF arc for the mixture.

The above shows that, for steel electrodes with electrochemically induced aragonite and calcite (two relevant allotropic forms of $CaCO_3$) scales immersed in the characterization medium, typical impedance diagrams (Figure 5(a) and (b), respectively) can be identified. Based on the shape of impedance diagrams only, the impedance response of the aragonite–calcite mixture seems to be dominated by the presence of aragonite in the scale and the differences between Figure 5(c) and (a) are most likely related to morphological and scale coverage features. In order to better explain this behaviour, the effect of formation time (extent of scale) was investigated for surfaces scaled with aragonite and with the mixture.

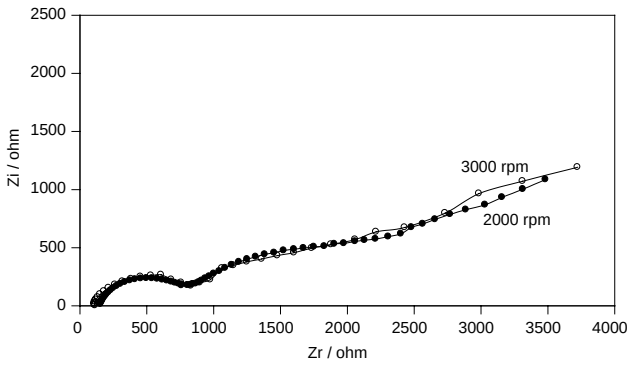

Fig. 6. Typical Nyquist diagrams obtained for the scaled carbon steel surface (aragonite previously grown for 10 min) in fresh solution AS3C (characterization medium), at different rotation rates. (a) 2000 rpm and (b) 3000 rpm.

3.3. *Effect of extent of scale for aragonite and the mixture*

Figures 7(a) and (b) shows the effect of the scale extent (different formation time) for steel surfaces scaled with aragonite and a mixture of aragonite–calcite, respectively. In each case the impedance measurement was carried out after 10 min stabilization in a fresh AS3C solution, a time sufficient to obtain a steady state at this interface. For aragonite (Figure 7(a)) and the mixture (Figure 7(b)), an increase in the extent of scaling led to an increase in the size of the HF arc and also to a shift in the MF and LF loops to the right in the real impedance axis. The scale with a mixture of aragonite–calcite seems

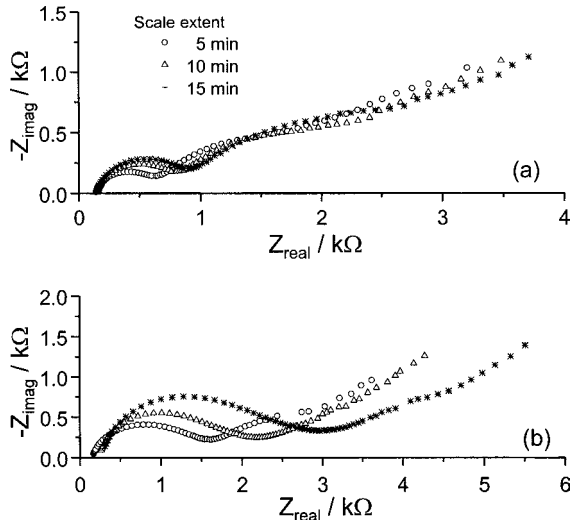

Fig. 7. Effect of scale formation time (scale extent) for surfaces that were scaled with: (a) aragonite and (b) calcite–aragonite mixture.

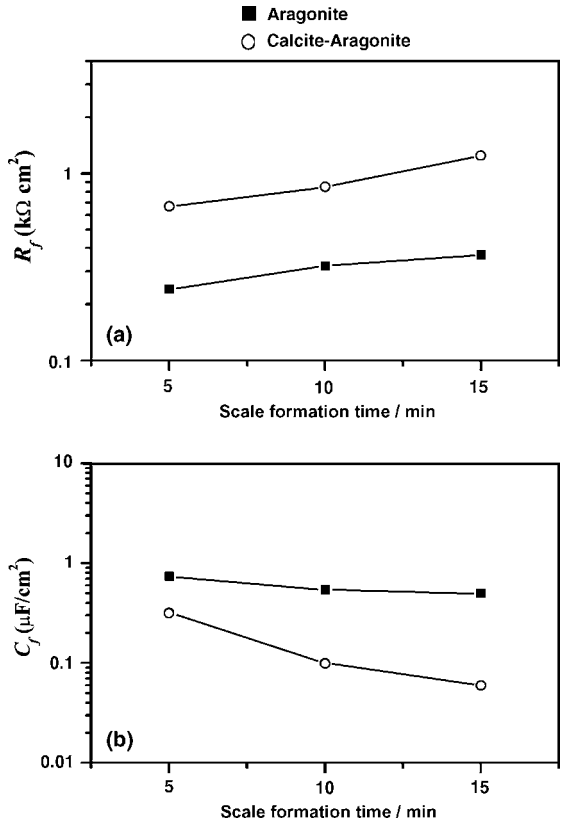

Fig. 8. Change with scale formation time (scale extent) of the resistance (a) and capacitance (b) of the aragonite and aragonite–calcite scale layers.

to be more sensitive to the effect of extent of scale than that of aragonite alone.

According to the analysis of the impedance response of aragonite in Figure 5(a), the HF arc for the mixture (Figure 7(b)) and aragonite (Figure 7(a)) scales can be attributed to the impedance of the scale layer itself. The MF loop corresponds to the reduction of oxygen in cavities under the scale and the LF loop to oxygen diffusion through the scale. To analyse the effect of extent of scaling for aragonite and the mixture, values for the resistance, R_f, and the capacitance, C_f, of the scales was estimated by fitting a semicircle through the HF loop. The film resistance, R_f, increases in both cases as the time of damage increases (Figure 8(a)), indicating a decrease in porosity. Moreover, the values are higher in the mixture than for aragonite, confirming that the presence of calcite crystals in the mixture leads to a more coherent scale. Variations in the film capacitance C_f can be associated with variations in the thickness of the scale layer. An increase in formation time leads to a decrease in C_f in both cases (Figure 8(b)), thus suggesting an increase in scale thickness; the effect was, however, more pronounced for the mixture than for the aragonite scales. It is also observed that at any formation time, C_f is smaller for the mixture, suggesting that the scale containing aragonite and calcite was thicker compared to that of aragonite alone.

The fact that the MF loop and the LF suffered little variations (in the shape and magnitude of impedance) with increasing formation time is in agreement with indications about the protective nature of the scale layers given by C_f and R_f.

To sum up, each of the scales investigated has a characteristic impedance response, which is different to that for a corrosion products layer. EIS could be used to differentiate two allotropic forms of calcium carbonate, aragonite and calcite. An analysis of features of the HF loop related to the morphology such as porosity, coherence and thickness of aragonite and aragonite–calcite deposits was made, and it was shown that the presence of calcite in the scale corresponding to the mixture rendered it more coherent and thicker with respect to the aragonite scale. Although the study of systems in which scale and corrosion process are simultaneously carried out is very complex, this work presents a first quantitative attempt to discern physical phenomena occurring in practical cooling water systems.

4. Conclusions

The results show that for the metal–water system investigated, typical electrochemical impedance diagrams for two relevant allotropic forms of calcium carbonate (calcite and aragonite) can be identified. In particular for the aragonite and aragonite–calcite scales, it was possible to determine parameters that are related to the morphology of the deposits, and which are in good agreement with SEM observations.

The impedance response of the scale with a calcite–aragonite mixture was dominated by the aragonite constituent. However, from the values of R_f, and C_f it could be determined that the calcite constituent had a strong influence on the scale morphology. The calcite crystals merged laterally with the aragonite agglomer-

ates to form a more coherent and thicker scale, compared to that for a scale consisting of aragonite alone. For scales containing aragonite and a calcite–aragonite mixture, increasing scaling time led to less porous and thicker deposits.

With regard to practical implications, two observations can be made in connection with the influence of the scale layers investigated in this work on: (a) the corrosion process of the carbon steel surface, and (b) the deposit thermal resistance. It is likely that a higher surface blockage in the case of the calcite–aragonite mixture results in a lower corrosion rate of the steel substrate. However, having the higher deposit mass per unit area, the mixture is expected to have a high thermal resistance.

Acknowledgements

J. Marín-Cruz and R. Cabrera-Sierra thank CONACyT for a graduate scholarship and the Molecular Engineering Program (IMP) for their aid in performing this study.

References

1. N. Andristos, A.J. Karabelas and P.G. Koutsoukos, *Langmuir* **13** (1997) 2873.
2. R. Jaouhari, A. Benbaghir, A. Guenbour, C. Gabrielli, J. García-Jareno and G. Maurin, *J. Electrochem. Soc.* **147** (2000) 2151.
3. C.W. Turner and D.W. Smith, *Ind. Eng. Chem. Res.* **37** (1998) 439.
4. N.H. de Leeuw and S.C. Parker, *J. Phys. Chem. B* **102** (1998) 2914.
5. C. Deslouis, C. Gabrielli, M. Keddam, A. Khalil, R. Rosset B. Tribollet and M. Zidoune, *Electrochim. Acta* **42** (1997) 1219.
6. C. Gabrielli, M. Keddam, A. Khalil, G. Maurin, H. Perrot, R. Rosset and M. Zidoune, *J. Electrochem. Soc.* **145** (1998) 2386.
7. C. Gabrielli, M. Keddam, A. Khalil, R. Rosset and M. Zidoune, *Electrochim. Acta* **42** (1997) 1207.
8. C. Gabrielli, M. Keddam, G. Maurin, H. Perrot, R. Rosset and M. Zidoune, *J. Electroanal. Chem.* **412** (1996) 189.
9. A. Neville, T. Hodgkiess and A.P. Morizot, *J. Appl. Electrochem.* **29** (1999) 455.
10. C. Gabrielli, G. Maurin, G. Poindessous and R. Rosset, *J. Cryst. Growth* **200** (1999) 236.
11. L. Beaunier, C. Gabrielli, G. Poindessous, G. Maurin and R. Rosset, *J. Electroanal. Chem.* **501** (2001) 41.
12. S. Xu, C.A. Melendres, J.H. Park and M.A. Kamrath, *J. Electrochem. Soc.* **146** (1999) 3315.
13. K.E. Mantel, W.H. Hartt and T.Y. Chen, *Corrosion* **48** (1992) 489.
14. J. Marín-Cruz, E. Garcíafigueroa, M. Miranda-Hernández and I. González, *Water Res.* **38** (2004) 173.
15. J. Marín-Cruz and I. González, *J. Electrochem. Soc.* **149** (2002) B1.
16. S-H. Lin and S.C. Dexter, *Corros. Sci.* **44** (1988) 615.
17. M.M. Kunjapur, W.H. Hartt and S.W. Smith, *Corrosion NACE* **43** (1987) 674.
18. M. Duprat, M.C. Lafont and F. Dabosi, *Electrochim. Acta* **30** (1985) 353.
19. L. Bousselmi, C. Fiaud, B. Tribollet and E. Triki, *Electrochim. Acta* **44** (1999) 4357.
20. C. Cachet and R. Wiart, *J. Electrochem. Soc.* **141** (1994) 131.
21. C. Cachet, I. Epelboin, M. Keddam and R. Wiart, *J. Electroanal. Chem.* **100** (1979) 745.
22. C. Cachet and R. Wiart, *J. Appl. Electrochem.* **20** (1990) 1009.